The Auk 117(4):1003–1015, 2000

MITOCHONDRIAL DNA PHYLOGENY AND SPECIATION IN THE TRAGOPANS

ETTORE RANDI,[1,5] VITTORIO LUCCHINI,[1] TARA ARMIJO-PREWITT,[2] REBECCA T. KIMBALL,[2,3] EDWARD L. BRAUN,[2,4] AND J. DAVID LIGON[2]

[1]*Istituto Nazionale per la Fauna Selvatica, Via Cà Fornacetta 9, 40064 Ozzano dell'Emilia (BO), Italy;*
[2]*Department of Biology, University of New Mexico, Albuquerque, New Mexico 87131, USA;*
[3]*Department of Evolution, Ecology and Organismal Biology, Ohio State University, Columbus, Ohio 43210, USA; and*
[4]*Department of Plant Biology, Ohio State University, Columbus, Ohio 43210, USA*

ABSTRACT.—We sequenced mitochondrial DNA (mtDNA) from cytochrome *b* (cyt *b*) and the control region (CR) for all five extant species in the genus *Tragopan*. We incorporated information on comparative patterns and rates of molecular evolution into phylogenetic analyses, using both a single-gene and a combined data approach. Sequence variability was distributed heterogeneously among the three domains of CR and the three codon positions of cyt *b*, but the two genes evolved at comparable rates, on average, and produced concordant topologies independent of the method used for phylogenetic reconstructions. Phylogenetic trees suggest that *Tragopan* includes two main evolutionary lineages grouping *caboti-temminckii* (clade A), and *blythii-satyra* (clade B). A shorter CR sequence from one museum sample could not consistently resolve the position of *T. melanocephalus*. The mtDNA phylogeny is better supported than alternative topologies inferred from morphological and behavioral traits and is compatible with a mechanism of allopatric speciation of *Tragopan* in two different episodes about 4 and 2 million years ago. In those periods, the vicariant events that might have fostered allopatric speciation of *Tragopan* are represented by landscape changes that affected the Indohimalayan region after the sudden rising of the Himalayas less then 8 million years ago, and by climatic fluctuations during the Pleistocene less than 2 million years ago. *Received 18 June 1999, accepted 30 May 2000.*

THE FIVE EXTANT species in the genus *Tragopan* (Phasianidae) are almost linearly distributed across an arc that includes the Himalayan range, northern Pakistan to Burma, the forested mountains of central and southeastern China from Yunnan to Zhejiang, and northeastern Burma and northern Vietnam (Fig. 1). Distributions are allopatric except for limited contact zones between *T. satyra* and *T. blythii molesworthi* in the eastern Himalayas (Bhutan), and between *T. temminckii* and *T. caboti guangxiensis* in south-central China at Guangxi (Cheng 1980; Fig. 1).

Adult male tragopans have conspicuous and highly diagnostic color patterns that allow straightforward species identification (Johnsgard 1986, McGowan 1994). In particular, males have bright naked cheeks, bright throat and gular lappets, and two erectile horns that can be inflated and expanded during courtship displays (Johnsgard 1986, McGowan 1994:469). The sexes are highly dimorphic (McGowan 1994), and females and yearlings have inconspicuous and similar plumages. Sexual dimorphism and highly ritualized, complex courtship displays are important signals in mate recognition by tragopans, and these traits could have had a role in speciation via sexual selection (Islam and Crawford 1996, 1998).

Allopatric distributions suggest that tragopans speciated by vicariant fragmentation of widespread ancestral populations fostered by geographic barriers to gene flow and divergent adaptation of the isolated populations (Mayr 1970). However, owing to extreme sexual dimorphism and complex courtship behaviors in the group, sexual selection (Møller and Cuervo 1998) also may have had a role in segregating populations in contact, thus producing a sequential set of parapatric species in the absence of geographic isolation. To date, an explicit phylogeny of tragopans has not been available except for hypotheses based on qualitative evaluation of plumage color (Johnsgard 1986) and comparative behavior (Islam and Crawford 1996, 1998).

In this paper, we analyze an alignment of about 2,341 nucleotides of mitochondrial DNA

[5] E-mail: met0217@iperbole.bo.it

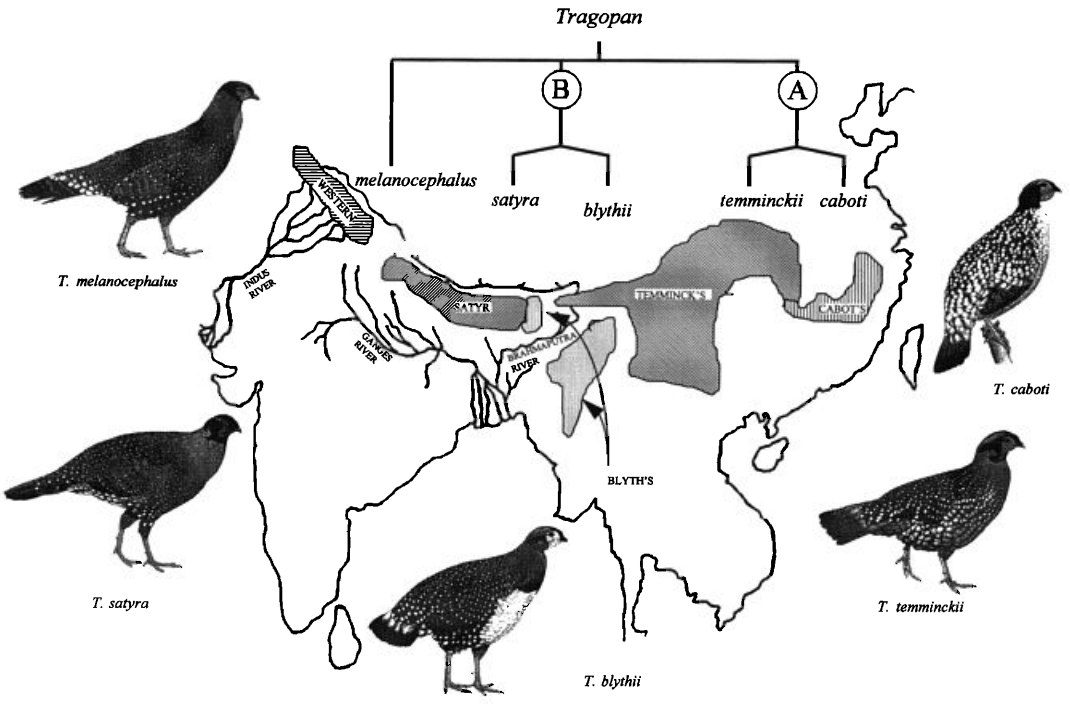

FIG. 1. Geographic distributions (Johnsgard 1986) and summary of phylogenetic relationships from cytochrome-*b* (cyt *b*) and control-region (CR) sequence analyses of the five extant species of *Tragopan* (drawings from McGowan [1994]). The phylogenetic tree summarizes concordant topologies obtained using maximum-parsimony, neighbor-joining, and maximum-likelihood methods. Values of internodal support for clades A and B are in Table 4. The phylogenetic position of *T. melanocephalus* was not fully resolved using the short CR sequence obtained by the available museum sample. The tree was rooted using cyt-*b* and CR sequences from *Pucrasia macrolopha, Ithaginis cruentus* and *Lophophorus impejanus* (not shown).

(mtDNA) that were sequenced from representatives of all five extant species of tragopans and from three phasianid outgroups. Phylogenetic analyses of these data are used to (1) describe the comparative patterns and rates of sequence evolution of the mtDNA control region (CR) and cytochrome-*b* (cyt *b*) genes and evaluate their phylogenetic utility; (2) produce a molecular phylogeny of the tragopans that can be used to assess the evolution of morphological and behavioral traits; and (3) correlate the inferred molecular phylogeny and extent of interspecific genetic divergence with Pliocene/Pleistocene biogeographical scenarios in the Himalayan region to suggest putative speciation patterns in *Tragopan*.

MATERIALS AND METHODS

DNA samples, PCR amplification, and sequencing.—We obtained samples (Table 1) from aviaries that maintain captive-reared stock of legal and documented geographic origins, except for *T. melanocephalus*, which is rare in nature and not reared in captivity outside of India. This species is represented by only one museum sample (A. Ghigi collection, INFS, Bologna).

Total DNA was extracted from 95% ethanol-preserved muscles or feather roots, using guanidinium thiocyanate and diatomaceous silica particles (Gerloff et al. 1995, Randi and Lucchini 1998) and a Puregene DNA isolation kit (Gentra Systems, Inc.; Kimball et al. 1999). In four species, the entire mtDNA CR and cyt-*b* genes were PCR amplified and sequenced as described by Randi and Lucchini (1998) and Kimball et al. (1999). Partial CR sequences (domain I) from the museum sample of *T. melanocephalus* were obtained by nested PCR. We used the primers PHDL and PH1H (Randi and Lucchini 1998) in the first amplification and PHDL with HimpDS1 (5′-TCATGGAGTACATTACGGGC-3′) in the semi-nested amplification. The museum sample was processed in a separate room dedicated only to ancient DNA. The absence of contamination was checked in all samples using negative controls during the extraction and

TABLE 1. Species names and GenBank accession numbers of *Tragopan* and outgroup samples used in this study.

Species	GenBank numbers	
	Control region	Cytochrome *b*
Tragopan caboti (Cabot's Tragopan)	AF230301, AF230302	AF200723
T. temminckii (Temminck's Tragopan)	AF230306, AF230307, AF230305	AF028802, AF229838
T. blythii (Blyth's Tragopan)	AF230300 (two identical sequences)	AF200722
T. satyra (Satyr Tragopan)	AF230303, AF230304	AF200724, AF229837
T. melanocephalus (Western Tragopan)	AF230311 (CR-375 nt)	—
Pucrasia macrolopha (Koklass Pheasant)	AF230310	AF028800
Ithaginis cruentus (Blood Pheasant)	AF230308	AF068193
Lophophorus impejanus (Himalayan Monal)	AF230309	AF028796

successive PCR amplifications. Additional phasianid outgroup sequences (*Pucrasia macrolopha, Ithaginis cruentus,* and *Lophophorus impejanus*) were obtained using the same PCR and sequencing methods.

Sequence analysis.—We aligned sequences with CLUSTAL W (Thompson et al. 1994) and edited alignments using Se-Al (A. Rambaut; <http://evolve.zoo.ox.ac.uk/Se-Al/Se-Al.html>). Nucleotide composition, variability at different positions and domains, and genetic distances were estimated using PAUP* (Swofford 1998). We performed a likelihood test for heterogeneity of substitution rates among CR and cyt-*b* domains using PLATO 2.01 (N. Grassly and A. Rambaut; <http://evolve.zoo.ox.ac.uk/Plato/Plato2.html>).

Sequences were analyzed both independently and combined. Phylogenetic congruence of combined cyt-*b* + CR sequences was assessed by a partition-homogeneity test (Farris et al. 1995) with 1,000 replicates, as implemented in PAUP*. Phylogenetic analyses were performed by PAUP* using (1) the neighbor-joining algorithm (NJ; Saitou and Nei 1987) with Tamura and Nei's (1993) DNA distance formula (TN93); (2) the exhaustive maximum-parsimony procedure (MP; Swofford 1998) with unordered and equally weighted characters, or with differential weighting of transversions (tv) over transitions (ti); and (3) the heuristic maximum-likelihood (ML) procedure (Felsenstein 1981). The best-fit ML model of DNA substitution was selected by likelihood-ratio tests among a suite of models of increasing complexity performed according to the following procedure (Huelsenbeck and Crandall 1997). First, we obtained the exhaustive MP trees using the cyt-*b* and CR sequences, either independently or combined; these topologies were identical and were used to compute the likelihood scores for substitution models of increasing complexity. Next, we assessed the best-fit models by the likelihood-ratio test:

$$\Delta = 2(\log L_1 - \log L_0), \quad (1)$$

where $\log L_1$ = likelihood of the most complex model and $\log L_0$ = likelihood of the simpler model. Values of Δ are distributed accordingly to a chi-square distribution (Huelsenbeck and Crandall 1997) and are used to determine whether simpler models should be rejected in favor of ones that are more complex.

We modeled substitution heterogeneity among sites by the discrete-rate γ distribution (Yang 1994). Values of the shape parameter α of the γ distributions, and ti/tv for cyt *b*, CR, and the combined sequences, were estimated by PAUP* using maximum likelihood with the best-fit substitution model and four discrete-rate categories.

We assessed the robustness of the phylogenies by bootstrap percentages (BP; Felsenstein 1988) computed using 1,000 random resamplings with replacement by PAUP*. Statistical differences among alternative phylogenetic trees were tested by Kishino and Hasegawa's (1989) likelihood and parsimony tests, and by Templeton's (1983) Wilcoxon test, as implemented in PAUP*.

RESULTS

*Comparative evolution of mtDNA CR and cyt-*b *genes.*—The average observed genetic distances (*p*-distances; Table 2) among the four species of tragopans were $D = 0.061 \pm$ SD of 0.011 for the cyt *b* and $D = 0.056 \pm 0.010$ for the CR. Intraspecific values of D ranged from 0.000 (between identical CR sequences of *T. blythii* and cyt *b* of *T. satyra*) to 0.013 between two CR sequences of *T. satyra.* Observed genetic distances between tragopans and the outgroups were $D = 0.122 \pm 0.018$ for cyt *b* and $D = 0.132 \pm 0.007$ for the CR.

Plotting of genetic distances (either proportional or corrected) of cyt *b* versus the CR suggested that the two genes evolved approximately at the same rate among tragopans and between tragopans and their outgroups (Fig. 2A), with the cyt *b* accumulating comparatively more ti but fewer tv than the CR (Fig. 2B). Cyt *b* evolved mainly by substitutions at third-co-

TABLE 2. Uncorrected proportional genetic distances (*p*-distances) among the studied *Tragopan* and outgroup species. Intraspecific CR/cyt-*b* distances are shown on the diagonal (not estimated in *T. caboti, T. blythii,* and the outgroups), interspecific CR distances are shown above the diagonal, and interspecific cyt-*b* distances are shown below the diagonal.

Species	1	2	3	4	5	6	7
1 *T. caboti*	0.0008/—	0.0389	0.0592	0.0631	0.1410	0.1310	0.1280
2 *T. temminckii*	0.0365	0.0070/0.0035	0.0625	0.0638	0.1376	0.1293	0.1306
3 *T. blythii*	0.0665	0.0675	0.0000/—	0.0507	0.1380	0.1359	0.1167
4 *T. satyra*	0.0674	0.0647	0.0586	0.0127/0.0000	0.1419	0.1424	0.1222
5 *P. macrolopha*	0.1111	0.1146	0.1181	0.1111	—	0.1276	0.1207
6 *I. cruentus*	0.1487	0.1435	0.1514	0.1373	0.1374	—	0.1078
7 *L. impejanus*	0.1102	0.1085	0.1137	0.1032	0.1067	0.1199	—

don positions (Figs. 3A and B, Table 3), in agreement with the well-known functional constraints of protein-coding genes (Irwin et al. 1991, Kumar 1996). The number of tv differences at first and second positions of cyt-*b* sequences was negligible in comparisons among tragopans and also among tragopans and the outgroups (Fig. 3B). Ti and tv accumulated at different rates in the three CR domains, and, in particular, ti leveled off faster in the hypervariable CR-I (Figs. 3D,E). Ti might saturate rapidly, but the CR seems to accumulate more tv at greater evolutionary distances than the cyt *b* (Figs. 3C,F).

Visual inspection of the sliding-window plot of the substitutions observed among tragopans (Fig. 4) suggested that sequence variability was distributed more homogeneously in the cyt *b* than in the CR. In fact, PLATO did not detect any cyt-*b* region evolving at significantly different rates based on a uniform substitution model. On the contrary, a region of 24 nucleotides in the second part of domain I, corresponding to hypervariable CR-IB as defined in the *Alectoris* partridges by Randi and Lucchini (1998), and a region of 214 nucleotides in the terminal part of domain III, evolved significantly faster than average in the CR (see also the proportions of variable sites in Table 3).

Quantitative data on nucleotide composition and variability showed that (1) the GC proportion was similar among inner, transmembrane, and outer cyt-*b* domains (Zhang et al. 1998) and among the three CR domains; (2) third-codon positions and domain IB were most variable in cyt *b* and CR, respectively; and (3) parsimony-informative sites were more frequent in cyt-*b* third-codon positions and cyt-*b* transmembrane, CR-IA, and CR-III domains (Table 3).

Testing models of DNA substitution.—For cyt *b*, CR, and the combined sequences, the best-fit model was the general time-reversible model (GTR; Lanave et al. 1984). The discrete γ distribution significantly improved the likelihood values over GTR with invariable sites ($P < 0.01$). Ti/tv ratios, estimated by ML with GTR + γ, were 6.22, 7.23, and 9.79 for cyt *b*, CR, and cyt *b* + CR sequences in *Tragopan* (without outgroups), respectively. These ratios were used for weighted maximum-parsimony analyses of cyt *b* (tv = 6 ti), CR (tv = 7 ti), and cyt *b* + CR (tv = 10 ti) alignments, respectively.

Phylogenetic relationships in tragopans.—Molecular, morphological, and behavioral data suggested that *Pucrasia, Ithaginis,* and *Lophophorus* are the most probable outgroups of *Tragopan* (Kimball et al. 1999). Using these three phasianids as outgroups, the genus *Tragopan* was clearly monophyletic (Fig. 5) despite the gene region and phylogenetic method used in phylogenetic analyses.

The phylogenetic trees computed by NJ, ML, and MP using nine individual tragopan CR sequences were identical to the topology in Figure 5 in showing a basal splitting of *Tragopan* into two clades that join the sister species *caboti-temminckii* (clade A) and *blythii-satyra* (clade B). Bootstrap values (Table 4) suggested that clade A (*caboti-temminckii*) was strongly supported independent of the method used in phylogenetic reconstruction, whereas clade B (*blythii-satyra*) received lower bootstrap support, particularly from equally weighted MP analyses of the CR (BP < 50%).

We obtained the same topology using the cyt-*b* sequences (one sequence from each species of *Tragopan*) or the combined cyt-*b* + CR alignment (the partition-homogeneity test was not significant; $P = 0.49$). Bootstrap support of clades A and B obtained with NJ, MP, and ML

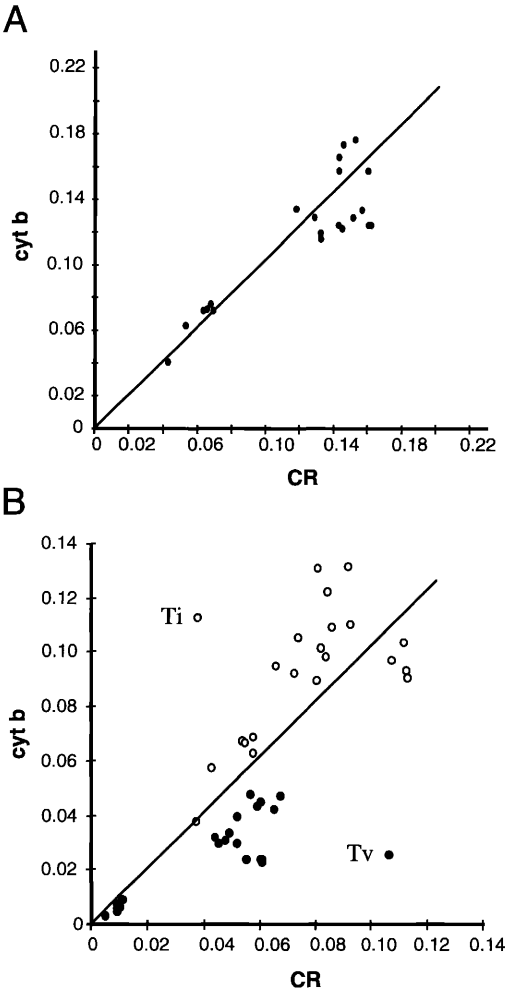

FIG. 2. (A) Pairwise cytochrome-*b* (cyt *b*) versus control-region (CR) TN93 DNA distances among *Tragopan* (lower left) and between *Tragopan* and the outgroups (upper right). (B) Cyt *b* versus CR percent differences among *Tragopan* and between *Tragopan* and the outgroups. Filled dots = transversions (tv); empty dots = transitions (ti). Diagonal lines indicate expected values given identical rates of substitutions in cyt-*b* and CR genes.

methods, and using cyt *b*, CR, and combined sequences (Table 4), indicated that (1) NJ analyses computed using TN93 or other distance models with both independent and combined sequences identified the two clades; however, the exclusion of highly variable transitions at third positions of cyt *b* disrupted the monophyly of the *blythii-satyra* clade (BP < 50%), and the exclusion of highly variable CR-IB disrupted the monophyly of the *caboti-temminckii* clade A (BP < 50%); (2) in equally weighted MP analyses, cyt *b* and the combined genes supported the two clades, whereas the *blythii-satyra* clade was not supported using the CR; (3) weighted MP analyses slightly improved the BP support of tragopan clade B (BP = 60%) using the CR; and (4) ML analyses performed with the GTR model and heterogenous substitution rates supported clades A and B in analyses of combined and separate data.

The museum sample of *T. melanocephalus* yielded degraded DNA, and we obtained only short sequences (375 nucleotides) of CR-I. Phylogenetic analyses performed using this partial data set associated *melanocephalus* with the *blythii-satyra* clade (Fig. 6A), although with low bootstrap support; alternative relationships of *melanocephalus* to the *caboti-temminckii* clade or to a basal unresolved polytomy also were possible (Figs. 6B,C). The topology shown in Figure 6A was the best one in terms of likelihood ($-\log L = 1{,}440.57$, with GTR + γ), but it did not differ significantly from the alternative trees (Figs. 6B,C) using the KH likelihood test (Table 5). This topology was shorter ($L = 223$ vs. 237 and 232) and significantly different ($P < 0.05$) from the alternatives using the KH parsimony and Templeton tests (Table 5). However, this topology had the same likelihood and length of trees representing alternative phylogenetic relationships among *Tragopan* (Johnsgard 1986; Islam and Crawford 1996, 1998; Figs. 6G,H). Thus, a better resolution of the relationships of *T. melanocephalus* will be possible when fresh samples become available for additional DNA sequencing.

Testing alternative phylogenetic hypotheses.— Johnsgard (1986) suggested that tragopans consisted of the superspecies *blythii-caboti* and *melanocephalus-satyra-temminckii* based on body size and plumage coloration. In contrast, based on quantitative analyses of vocalizations and qualitative comparisons of courtships displays, Islam and Crawford (1996, 1998) suggested that "the centrally distributed species of tragopans (Satyr, Blyth's and Temmink's) retained characteristics of the ancestral population. . . ." and were closely related to each other, whereas "the peripheral species (Western and Cabot's) underwent vocal modifications. . . ." and were separated into two distinct groups. The different phylogenies underlying morphological, behavioral, and mtDNA data are shown in Figure

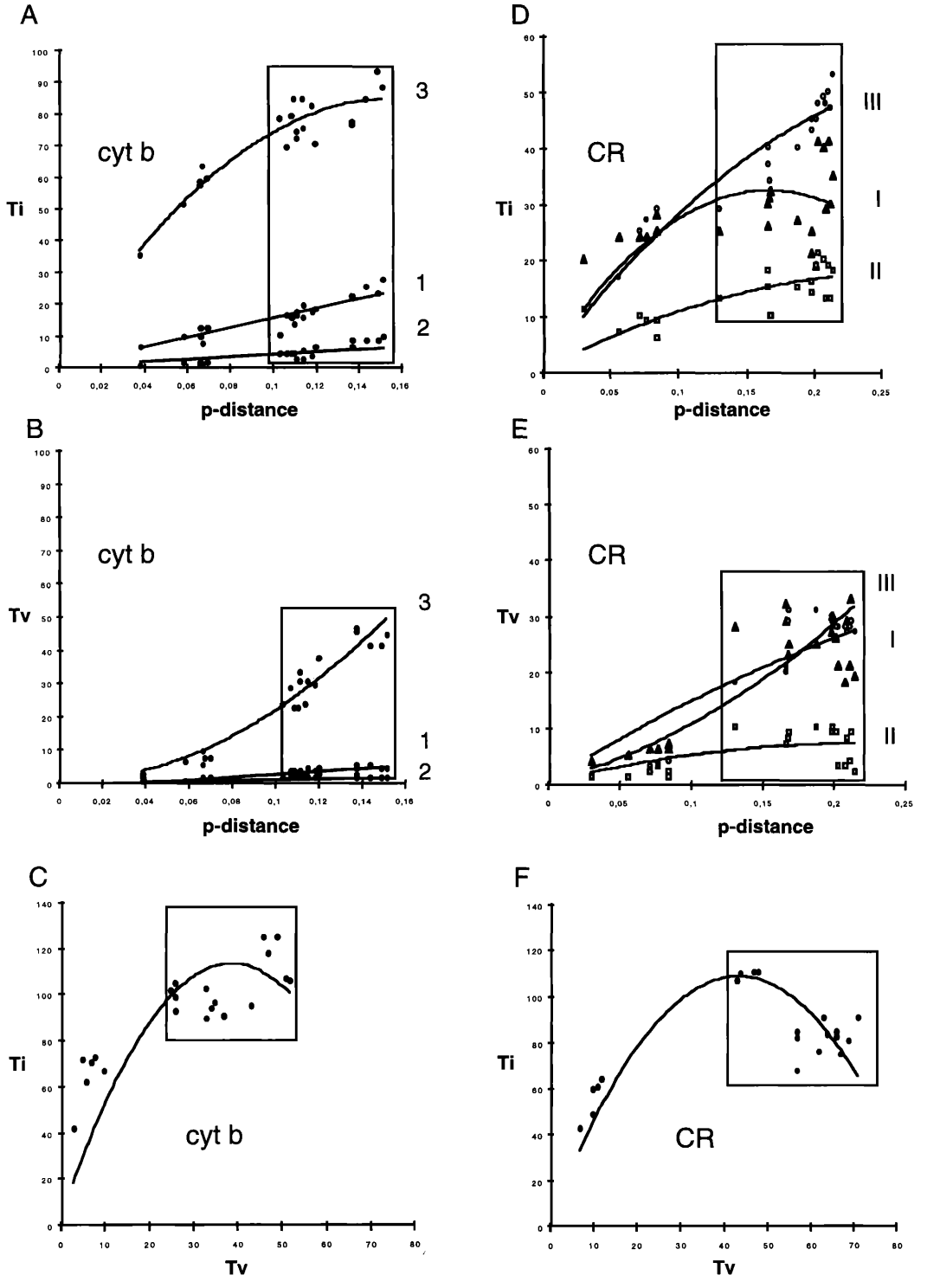

FIG. 3. (A) Cyt-*b* transitions (ti) and (B) transversions (tv) versus uncorrected proportional DNA distances (*p*-distances); (C) cyt-*b* ti versus tv; (D) number of CR ti; (E) tv versus percent pairwise DNA distances; and (F) ti versus tv in *Tragopan* and their outgroups (in box). First, second, and third cyt-*b* codon positions are

TABLE 3. Nucleotide composition and sequence variability at first, second, and third cyt-*b* codon positions; at inner, transmembrane (trans) and outer cyt-*b* domains (Zhang et al. 1998); and at IA, IB, II, and III control-region domains (Randi and Lucchini 1998).

	Cytochrome *b*						Control region			
	1st	2nd	3rd	Inner	Trans	Outer	IA	IB	II	III
Nucleotides	381	381	381	228	585	330	163	154	468	397
GC proportion	0.50	0.39	0.50	0.43	0.48	0.47	0.38	0.40	0.50	0.30
% Variable[a]	0.05	0.003	0.28	0.13	0.10	0.11	0.08	0.28	0.04	0.11
% Parsimony[b]	0.22	0.00	0.27	0.17	0.30	0.26	0.31	0.23	0.26	0.40

[a] Proportion of total nucleotides that are variable.
[b] Proportion of variable nucleotides that are parsimony informative.

6, and statistical significance of the topologies has been analyzed using KH and Templeton tests (Table 5). The mtDNA phylogeny (Fig. 6D) represents the best explanation of the data using the total cyt-*b* + CR alignment without *T. melanocephalus*. The alternative topologies proposed by Islam and Crawford (Fig. 6E) and Johnsgard (Fig. 6F) are different from the mtDNA phylogeny at $P < 0.0001$ (Table 5). Using only the short alignment of 375 nucleotides including *T. melanocephalus*, the alternative phylogenies (Figs. 6G,H) were not significantly different from the best mtDNA topology (Fig. 6A).

DISCUSSION

*Evolution of CR and cyt-*b *genes, and phylogenetic inference.*—The evolution of mitochondrial genes is conditioned by peculiar functional constraints that define the number of sites that are free to vary and the kind of mutations that can be fixed, thus determining their total divergence rates (Zardoya and Meyer 1996). On average, CR and cyt *b* evolved at similar rates among tragopans and their outgroups over genetic distances ranging from 4 to 16% (see Fig. 2A, Table 2). These findings are in apparent contrast with the expected evolution of CR, which should be faster at early and slower at higher divergence levels owing to an inherently fast rate of evolution and rampant saturation of hypervariable sites and domains (Zhu et al. 1994, Lyrholm et al. 1996). However, in tragopans and the phasianid outgroups in this study, cyt *b* accumulated more ti but fewer tv differences than the CR (Fig. 2B). It is well known that most ti, particularly at third-codon positions, are synonymous and can evolve and saturate rapidly (Irwin et al. 1991). Thus, cyt-*b* sites that are free to vary tend to accumulate ti, which contribute the bulk of divergence at early intraspecific evolutionary steps but might saturate rapidly (Fig. 3C). The CR evolves rather conservatively, on average, and hypervariable sites are confined in two short regions at CR-IB and in the final part of CR-III domains (Fig. 4). The CR positions that are free to mutate can accept more tv than cyt *b*, thus continuing to accumulate mutations at greater evolutionary distances (Fig. 3F). That is why, rather surprisingly, avian CRs express substantial phylogenetic signal and can be used for phylogenetic inference in a relatively wide window of evolutionary divergence (Kimball et al. 1997, 1999; Kidd and Friesen 1998; Randi and Lucchini 1998).

Variable rates of substitution at different sites and domains require that complex models of DNA evolution be used for phylogenetic inference of mtDNA sequences (Tamura and Nei 1993, Yang 1996). In this case, the best-fit maximum-likelihood model had the most parameters, the GTR. Complex evolutionary models increase the variance of the estimated parameters and therefore require longer sequences to increase the probability of obtaining well-supported (although not necessarily correct) phylogenies. Phylogenetic relationships among tragopans can be reliably reconstructed with

←

indicated as 1, 2, and 3. The three CR domains are indicated as I, II, and III. Ti and tv numbers are not independent from the estimated DNA distances, so fitted second-order polynomials are intended to show trends of the plot and not to analyze their statistical properties.

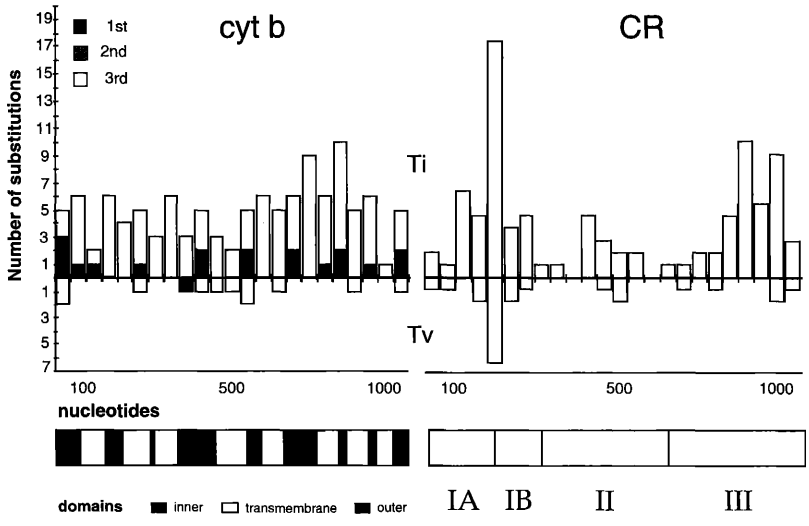

FIG. 4. Variability at first-, second-, and third-codon positions in inner, transmembrane, and outer domains of cyt *b* (after Zhang et al. 1998) and in CR domains IA, IB, II, and III (after Randi and Lucchini 1998) plotted along a nonoverlapping sliding window of 50 nucleotides in *Tragopan*.

shorter sequences, but the combined cyt-*b* + CR alignment consistently produced the strongest internodal support values (Table 4). Despite the suspected increase of homoplasy at hypervariable sites and domains, the signal expressed by CR-IB and third-position ti of cyt *b* helped to improve the resolution of the tragopan phylogeny (see also Kimball et al. 1999). Although saturation plots are often used to determine rapidly evolving sites that are more likely to be saturated, saturation in itself does not preclude phylogenetic information.

Phylogenetic relationships of tragopans and taxonomic implications.—The cyt-*b* + CR sequences identified two unambiguous clades in *Tragopan*, the first joining *temminckii* and *caboti* (clade A) and the second one joining *satyra* and *blythii* (clade B). However, the partial CR-I *melanocephalus* sequence obtained from a feather sample did not firmly resolve the relationships of this species. The mtDNA phylogeny was not concordant with the two superspecies of Johnsgard (1986), i.e. *melanocephalus-satyra-temminckii* and *blythii-caboti*, nor with the central versus pe-

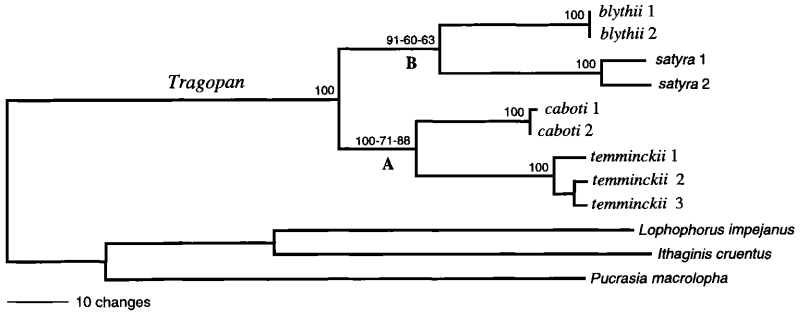

FIG. 5. Phylogenetic tree of nine individual CR sequences from four species of *Tragopan* and three phasianid outgroups. Tree computed by PAUP* using the heuristic maximum-likelihood procedure with the GTR model (log $L = -3{,}771.99$). Values of ti / tv (2.15) and the shape parameter α (0.22) of a discrete γ distribution with four categories were estimated from the data. Identical topologies were obtained by NJ and MP methods using either the CR, cyt-*b*, or the combined cyt-*b* + CR sequences. Values of bootstrap support computed using NJ (with TN93 genetic distances; other distance models produced identical results), weighted MP (with tv = 7ti), and ML (with GTR + γ model) are reported above internodes of tree. Other bootstrap values for clades A and B are reported in Table 4.

TABLE 4. Percent bootstrap support for *Tragopan* clade A (*caboti-temminckii*) and clade B (*blythii-satyra*) from phylogenetic analyses using neighbor-joining with Tamura-Nei (TN93) genetic distances, equally weighted and weighted maximum-parsimony methods, and maximum-likelihood method with the GTR model and discrete γ-distributed substitution rates (four categories). Weighted maximum-parsimony analyses were performed using tv = 6ts, tv = 7ts, and tv = 10ts for cyt *b*, CR, and combined sequences, respectively. Phylogenetic analyses were performed with nine individual *Tragopan* CR and four individual cyt *b* and combined *Tragopan* sequences.

Model	Sequence[a]	Clade A	Clade B
Neighbor joining			
TN93	cyt *b*	100	74
	cyt *b*-3	88	<50
	CR	100	91
	CR-IB	<50	68
	cyt *b* + CR	100	96
Maximum parsimony			
Equally weighted	cyt *b*	97	78
	CR	95	<50
	cyt *b* + CR	100	82
Weighted	cyt *b*	93	93
	CR	71	60
	cyt *b* + CR	95	93
Maximum likelihood			
GTR $\gamma_{(4)}$	cyt *b*	88	68
	CR	87	68
	cyt *b* + CR	96	94

[a] Sequences: cyt *b* = cytochrome *b*; cyt *b*-3 = cyt *b* excluding third-codon positions; CR = control region; CR-IB = CR excluding hypervariable domain IB; cyt *b* + CR = cyt *b* = CR combined.

ripheral species groups, i.e. *satyra-blythii-temminckii* versus *melanocephalus* and *caboti* as indicated by analyses of vocalizations and behavior (Islam and Crawford 1996, 1998).

Biogeography and speciation in tragopans.—The topology of the molecular tree overlaps the present geographic distribution of tragopans (Fig. 1). The observed phylogenetic pattern is compatible with a mechanism of allopatric speciation and could have been generated either by fragmentation of a widespread ancestral population, or by dispersal and divergence along the Himalayan and central Chinese mountain ranges. Johnsgard (1986) postulated the existence of a major center of origin of pheasant diversity in the eastern Himalayas and across northern Burma and Yunnan. The hypothetical ancestral populations could have been located in this area and were then progressively fragmented or dispersed, producing the western and the eastern tragopan lineages that spread toward the Himalayas and central and southeastern China, respectively.

The two main clades of tragopans diverged at about 8% cyt-*b* genetic distance, which could have been generated in a time span of about 4 million years, assuming the standard rate of vertebrate mtDNA evolution of 2% per million years (Avise and Walker 1998). Thus, the first evolutionary split could have been fostered by the dramatic consequences of the sudden uplifting of the Himalayas less than 8 million years ago (Harrison et al. 1992, Abdrakhmatov et al. 1996), which created a series of parallel mountain ranges running from east to west (and from north to south in Pakistan and Burma), thus inducing the first basal split among the Himalayan and Chinese ancestors of extant tragopans. The Himalayas continued to rise throughout the Pliocene and Pleistocene and forced the pre-existing main fluvial watersheds to cut deep canyons through the mountain valleys. Present distributions of Himalayan tragopans are bounded by some of the major fluvial watersheds of the area (Johnsgard 1986); e.g. the distribution of *T. melanocephalus* corresponds to the basin of the Indus River, *T. satyra* inhabits the entire watershed of the Ganges River, and *T. blythii* occurs on the western (*T. b. blythii*) and eastern (*T. b. molesworthi*; known only from three specimens) sides of the Brahamaputra River (Fig. 1).

The rising of the Himalayas also had major climatic consequences (Cracraft 1973). For example, the warm tropical climate of the Tibetan Plateau changed rapidly, and formerly uniform tropical forests shifted to the humid southern slopes and disappeared from the arid northern slopes and internal valleys. Habitat diversification followed an obvious vertical gradient and an east-west gradient, with the monsoon rains being heaviest on the eastern side of the Himalayas and the west being arid (Shaller 1977). Further major habitat changes in the Himalayas have been produced by Pleistocene glacial/interglacial cycles. Ice sheets expanded in the Himalayas during glacial periods with consequent elevational shifting of steppes and forests and cyclic fluctuations in the distributions of animals.

The cyt-*b* sequence divergence between sister species of *Tragopan* is 3.6% (clade A) and 5.9% (clade B), corresponding to about 1.8 to 2.9 million years of evolutionary divergence. Thus,

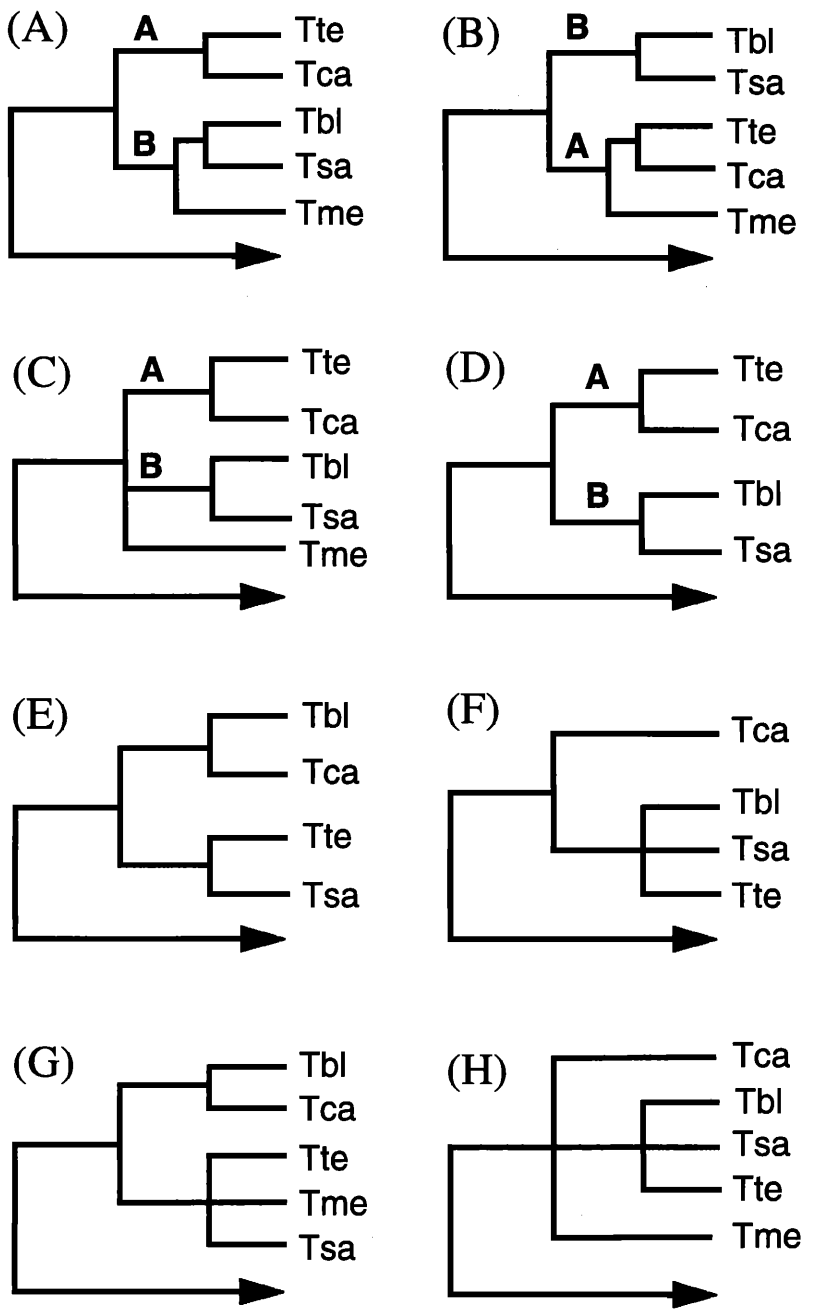

FIG. 6. Alternative relationships of *Tragopan melanocephalus* resulting from phylogenetic analyses of 375 nucleotides of CR-I sequences (A, B, and C). The first tree (A) is significantly better than the alternatives (B and C) using likelihood or parsimony testing (Table 5). Tree D represents the phylogeny of *Tragopan* as obtained in this study based on the entire cyt-*b* and CR sequences. Alternative phylogenies proposed by Islam and Crawford (1996, 1998) based of vocalizations and courtship displays, and Johnsgard (1986) based on external morphology, are represented in trees E and F, respectively. The molecular tree (D) is significantly better than the alternatives (E and F), using likelihood or parsimony testing (Table 5). Trees G and H correspond to Islam and Crawford's and Johnsgard's phylogenies and include *T. melanocephalus*. Using the short CR-I sequence available for *T. melanocephalus*, trees G and H have the same likelihood ($-\log L = 1{,}440.57$)

TABLE 5. Results of the likelihood and parsimony testing of alternative relationships of *Tragopan melanocephalus* (A, B, and C) estimated using 375 nucleotides of CR-I, and alternative phylogenies of *Tragopan*, as proposed in this study based on the entire mtDNA cyt-*b* and CR sequences (D), by Islam and Crawford (1996, 1998), and (E) by Johnsgard (1986) (F). The topologies of these trees are represented in Figure 6. Likelihood tests were performed using the GTR + γ model, with parameters estimated from the data. Parsimony tests were performed using all characters unordered and equally weighted.

	Likelihood test		Parsimony test		
Trees	$-\log L$	KH *P*	Length	KH *P*	Templeton *P*
A	1,440.57	Best	223	Best	Best
B	1,450.62	0.08	237	<0.05	<0.05
C	1,450.96	0.07	232	<0.05	<0.05
D	7,035.20	Best	845	Best	Best
E	7,089.75	<0.0001	886	<0.0001	<0.0001
F	7,089.75	<0.0001	891	<0.0001	<0.0001

speciation in *Tragopan* might have been fostered by events in the Pliocene and Pleistocene, which split the Himalayan populations into western *melanocephalus*, central *satyra*, and eastern *blythii* and split the Chinese populations into western *temminckii* and eastern *caboti*.

Sexual selection and speciation in tragopans.—A phylogenetic tree similar to the one expected from geographic speciation through vicariance also could be produced by parapatric speciation driven by sexual selection. In this case, the phenotypic traits selected during parapatric speciation owing to sexual selection should be phylogenetically informative (Brooks and McLennan 1991).

However, this is not the case in tragopans. The lack of concordance between the phylogenetic patterns and the distribution of phenotypic traits likely to be subject to sexual selection is illustrated by lappet morphology. All five tragopans possess inflatable blue horns and large frontal lappets or bibs. In three species (*satyra, temminckii*, and *melanocephalus*) belonging to both major branches of the molecular phylogeny (Fig. 1), the primary colors adorning the lappet are blue and red (Johnsgard 1986, McGowan 1994:469). In two others (*blythii* and *caboti*), also occupying different phylogenetic branches, the lappets are largely yellow or orange (although small amounts of blue coloration occur in each of these species). Given the distribution of color patterns, it is likely that blue and red evolved initially, and that orange/yellow coloration evolved independently in each lineage.

This evolutionary model assumes that a lappet-like structure occurred in the common ancestor of the five species, and as each population became isolated, female preferences selected for unique color patterns that provided information about the quality of a given male relative to other males. The lappets of male tragopans possess features that may signal male health or quality. For example, if the yellow and red on the lappets of all five tragopan species are based on carotenoid pigments, then the lappets have the potential to signal condition, as seen in some other avian species (e.g. Ligon 1999). In addition, the patterns of four of the five species (all but *blythii*) exhibit bilateral symmetry in color pattern. Bilateral symmetry, like carotenoids, is thought to provide a mechanism for signaling quality (Ligon 1999). The lappets of all tragopans except *blythii* appear to be beautifully designed to emphasize symmetric development of color patterns.

The allopatric distributions and the pattern of phylogenetic relationships among tragopans, together with the idiosyncratic distribution of phenotypic traits likely to be under sexual selection, provide evidence against sympatric speciation. Taken together, molecular phylogeny, geographic distribution, and behavior suggest that tragopans evolved in allop-

←

and length (L = 223) and are not statistically different from tree A. Tsa = *T. satyra*; Tme = *T. melanocephalus*; Tte = *T. temminckii*; Tbl = *T. blythii*; Tca = *T. caboti*. Trees were rooted using sequences from *Pucrasia macrolopha, Ithaginis cruentus*, and *Lophophorus impejanus* (not shown).

atry by vicariance owing to historical fragmentation and extrinsic barriers to gene flow. Other species that evolved in the same periods and that share similar habitats should have been affected by the same biogeographic factors promoting isolation and speciation. It is worth noting that closely related *Lophophorus impejanus* and *L. sclateri* and *Lophura leucomelanos* and *L. nycthemera* have distributions similar to clades A and B of *Tragopan* (Johnsgard 1986, McGowan 1994), indicating that a main split between Himalayan versus Chinese pheasant populations might have been generated by common biogeographic factors.

ACKNOWLEDGMENTS

This work was supported by the Istituto Nazionale per la Fauna Selvatica (INFS) and by NSF through the RIMI molecular biology facility at the University of New Mexico. We thank A. Hennache (Parc Zoologique de Clères, France), M. Kaiser (Tierpark Berlin, Germany), R. Sumner (Triple S Game Farm, USA), and S. Latimer for kindly providing us with tissue samples. F. H. Sheldon, T. Crowe, and an anonymous reviewer provided helpful comments that improved an early draft of this paper. We deeply appreciate the editorial help provided by J. S. Marks.

LITERATURE CITED

ABDRAKHMATOV, K. Y., S. A. ALDAZHANOV, B. H. HAGER, M. W. HAMBURGER, T. A. HERRING, K. B. KALABAEV, V. I. MAKAROV, P. MOLNAR, S. V. PANASYUK, M. T. PRILEPIN, R. E. REILINGER, I. S. SADYBAKASOV, B. J. SOUTER, YU. A. TRAPEZNIKOV, V. Y. TSURKOV, AND A. V. ZUBOVICH. 1996. Relatively recent construction of the Tien Shan inferred from GPS measurements of present-day crustal deformation rates. Nature 384:450–453.

AVISE, J. C., AND D. WALKER. 1998. Pleistocene phylogeographic effects on avian populations and the speciation process. Proceedings of the Royal Society of London Series B 265:457–463.

BROOKS, D. R., AND D. A. MCLENNAN. 1991. Phylogeny, ecology, and behavior: A research program in comparative biology. University of Chicago Press, Chicago.

CHENG, T. H. 1980. A new subspecies of *Tragopan caboti*: *Tragopan caboti guangxiensis*. Page 43 *in* Proceedings of the International Symposium of Pheasants in Asia (C. D. W. Savage, Ed.). World Pheasant Association, Basildon, United Kingdom.

CRACRAFT, J. C. 1973. Continental drift, paleoclimatology, and the evolution and biogeography of birds. Journal of Zoology (London) 169:455–545.

FARRIS, J. S., M. A. KALLERSJÖ, G. KLUGE, AND C. BULT. 1995. Testing significance of incongruence. Cladistics 10:315–319.

FELSENSTEIN, J. 1981. Evolutionary trees from DNA sequences: A maximum likelihood approach. Journal of Molecular Evolution 17:368–376.

FELSENSTEIN, J. 1988. Phylogenies from molecular sequences: Inference and reliability. Annual Review of Genetics 22:521–565.

GERLOFF, U., C. SCHLOTTERER, K. RASSMANN, I. RAMBOLD, G. HOHMANN, B. FRUTTH, AND D. TAUTZ. 1995. Amplification of hypervariable simple sequence repeats (microsatellites) from excremental DNA of wild living bonobos (*Pan paniscus*). Molecular Ecology 4:515–518.

HARRISON, T. M., P. COPELAND, W. S. F. KIDD, AND A. YIN. 1992. Raising Tibet. Science 255:1663–1670.

HUELSENBECK, J. P., AND K. A. CRANDALL. 1997. Phylogeny estimation and hypothesis testing using maximum likelihood. Annual Review of Ecology and Systematics 28:437–466.

IRWIN, D. M., T. D. KOCHER, AND A. C. WILSON. 1991. Evolution of the cytochrome *b* gene of mammals. Journal of Molecular Evolution 32:128–144.

ISLAM, K., AND J. A. CRAWFORD. 1996. A comparison of four vocalizations of the genus *Tragopan* (Aves, Phasianidae). Ethology 102:481–494.

ISLAM, K., AND J. A. CRAWFORD. 1998. Comparative displays among four species of tragopans and their derivation and function. Ethology, Ecology and Evolution 10:17–32.

JOHNSGARD, P. A. 1986. The pheasants of the world. Oxford University Press, Oxford.

KIDD, M. G., AND V. L. FRIESEN. 1998. Analysis of mechanisms of microevolutionary change in *Ceppus* guillemots using patterns of control region variation. Evolution 52:1158–1168.

KIMBALL, R. T., E. L BRAUN, AND J. D. LIGON. 1997. Resolution of the phylogenetic position of the Congo Peafowl, *Afropavo congensis*: A biogeographic and evolutionary enigma. Proceedings of the Royal Society of London Series B 264: 1517–1523.

KIMBALL, R. T., E. L. BRAUN, P. W. ZWARTJES, T. M. CROWE, AND J. D. LIGON. 1999. A molecular phylogeny of the pheasants and partridges suggests these lineages are polyphyletic. Molecular Phylogenetics and Evolution 11:38–54.

KISHINO, H., AND M. HASEGAWA. 1989. Evaluation of the maximum likelihood estimate of the evolutionary tree topologies from DNA sequence data, and the branching order in Hominoidea. Journal of Molecular Evolution 29:170–179.

KUMAR, S. 1996. Patterns of nucleotide substitution in mitochondrial protein coding genes of vertebrates. Genetics 143:537–548.

LANAVE, C., G. PREPARATA, C. SACCONE, AND G. SERIO. 1984. A new method for calculating evolu-

tionary substitution rates. Journal of Molecular Evolution 20:86–93.

LIGON, J. D. 1999. The evolution of avian breeding systems. Oxford University Press, Oxford.

LYRHOLM, T., O. LEIMAR, AND U. GYLLENSTEN. 1996. Low diversity and biased substitution patterns in the mitochondrial DNA control region of sperm whales: Implications for the estimates of time since common ancestry. Molecular Biology and Evolution 13:1318–1326.

MAYR, E. 1970. Populations, species and evolution. Harvard University Press, Cambridge, Massachusetts.

MCGOWAN, P. J. K. 1994. Family Phasianidae. Pages 434–557 *in* Handbook of the birds of the world, vol. 2 (J. del Hoyo, A. Elliott, and J. Sargatal, Eds.). Lynx Edicions, Barcelona.

MØLLER, A. P., AND J. J. CUERVO. 1998. Speciation and feather ornamentation in birds. Evolution 52: 859–869.

RANDI, E., AND V. LUCCHINI. 1998. Organization and evolution of the mitochondrial DNA control-region in the avian genus *Alectoris*. Journal of Molecular Evolution 47:449–462.

SAITOU, N., AND M. NEI. 1987. The neighbor-joining method: A new method for reconstructing phylogenetic trees. Molecular Biology and Evolution 4:406–425.

SHALLER, G. B. 1977. Mountain monarchs. University of Chicago Press, Chicago.

SWOFFORD, D. L. 1998. PAUP*: Phylogenetic analysis using parsimony (and other methods), version 4.0b2a. Sinauer Associates, Sunderland, Massachusetts.

TAMURA, K., AND M. NEI. 1993. Estimation of the number of nucleotide substitutions in the control region of mitochondrial DNA in humans and chimpanzees. Molecular Biology and Evolution 10:512–526.

TEMPLETON, A. R. 1983. Convergent evolution and non-parametric inferences from restriction fragment and DNA sequence data. Pages 151–179 *in* Statistical analysis of DNA sequence data (B. Weir, Ed.). Marcel Dekker, New York.

THOMPSON, J. D., D. G. HIGGINS, AND T. J. GIBSON. 1994. CLUSTAL W: Improving the sensitivity of progressive multiple sequence alignment through sequence weighting, position-specific gap penalties and weight matrix choice. Nucleic Acids Research 22:4673–4680.

YANG, Z. 1994. Maximum likelihood phylogenetic estimation from DNA sequences with variable rates over sites: Approximate methods. Journal of Molecular Evolution 39:306–314.

YANG, Z. 1996. Among-site rate variation and its impact on phylogenetic analyses. Trends in Ecology and Evolution 11:367–372.

ZARDOYA, R., AND A. MEYER. 1996. Phylogenetic performance of mitochondrial protein-coding genes in resolving relationships among vertebrates. Molecular Biology and Evolution 13:933–942.

ZHANG, Z., L. HUANG, V. M. SHULMEISTER, Y.-I. CHI, K. K. KIM, L.-W. HUNG, A. R. CROFTS, E. A. BERRY, AND S.-H. KIM. 1998. Electron transfer by domain movement in cytochrome bc_1. Nature 392: 677–684.

ZHU, D., B. G. M. JAMIESON, A. HUGALL, AND C. MORITZ. 1994. Sequence evolution and phylogenetic signal in D-loop and cytochrome *b* sequences of rainbow fishes (Melanotaeniidae). Molecular Biology and Evolution 11:672–683.

Associate Editor: F. H. Sheldon